

Experimental Measurement of Vapor Pressures and Densities of Pure Hexafluoropropylene

Christophe Coquelet,^{†,‡} Deresh Ramjugernath,^{*,‡} Hakim Madani,[§] Alain Valtz,[†] Paramespri Naidoo,[‡] and Abdeslam Hassen Meniai[§]

Mines ParisTech, Centre Energétique et Procédés, CEP/TEP 35 Rue Saint Honoré, 77305 Fontainebleau, France, Thermodynamics Research Unit, School of Chemical Engineering, University of KwaZulu-Natal, Durban, 4041, South Africa, and Laboratoire de L'ingénierie des Procédés D'environnement, Université Mentouri Constantine, Algérie

Hydrofluoroalkenes, like hexafluoropropylene, can be considered as new fluids for refrigeration systems, and consequently volumetric and critical property data are required. In this study a vibrating-tube densitometer technique was used to determine densities at 10 different temperatures between (263 and 362) K and pressures between (0.0009 and 10) MPa. The experimental uncertainties are ± 0.0005 MPa for pressure, ± 0.02 K for the temperature, and $\pm 0.05\%$ for vapor and liquid densities. Critical properties have been determined by direct measurement and utilization of experimental densities considering scaling laws. The Wagner, Span and Wagner, Peng–Robinson, and translated Peng–Robinson equations of state are used to correlate the data.

Introduction

Because of their global warming potential (GWP), hydrofluorocarbons (HFCs) will probably soon be phased out. Historically, they were used because of their zero ozone depletion potential (ODP). Prior to their use, chlorofluorocarbons (CFCs) and hydrochlorofluorocarbons (HCFCs) were used, but research indicated that they led to damage of the Earth's ozone layer, and they were ultimately banned. HFCs, which do not contain chlorine, pose no threat to the ozone layer, but due to their high stability, they have a high GWP (for example, the GWP of R134a is 1300¹). This has forced the refrigeration industry (domestic, cars, heat pumps) to consider and find alternate HFCs which have a much lower GWP. One solution could be the utilization of hydrofluoroalkenes, like hexafluoropropene (HFP, R1216, CAS Number 116-15-4). The GWP of HFP is 0.86,² which is negligible in comparison with the GWP of R134a.

In this paper, a complete study of volumetric properties of pure HFP determined using the vibrating-tube densitometer technique³ is presented. Pure component vapor pressures were also measured and critical properties determined from these and density measurements. The Span–Wagner,⁴ Peng–Robinson⁵ (PR EoS), and volume-translated Peng–Robinson⁶ equations of state were used to correlate the density data.

Experimental Section

Vapor-Pressure Apparatus. A classical static sapphire tube cell was used for the determination of pure HFP vapor pressures. It is similar to the cell used by Coquelet et al.⁷ Temperatures are measured by two Pt100 probes connected to a HP34970A data acquisition unit. These Pt100 probes were periodically calibrated against a $25\ \Omega$ reference thermometer (Tinsley Precision Instrument) certified by the Laboratoire National d'Essais (Paris, France).

* Corresponding author. E-mail: ramjuger@ukzn.ac.za. Telephone: +27 (0) 31 260 3128. Fax: +27 (0) 31 260 1118.

[†] Mines ParisTech, Centre Energétique et Procédés, CEP/TEP.

[‡] University of KwaZulu-Natal.

[§] Université Mentouri Constantine.

The resulting uncertainties on temperature measurements are within ± 0.02 K. Pressures were measured using a pressure transducer (model: Druck PTX611) with a pressure range of (0 to 4) MPa. The pressure transducer was calibrated against a dead weight pressure balance (model: Desgranges & Huot model 5202S) which has a (0.3 to 40) MPa pressure range. The pressure transducer is connected to the HP34970A data acquisition unit. The resulting uncertainties in pressure measurements are within ± 0.0005 MPa.

Vibrating-Tube Densimeter Apparatus. A detailed description of a typical vibrating-tube density measurement apparatus is given in a previous publication (Bouchot and Richon³). The apparatus used in this work uses an Anton Paar DMA 512 vibrating tube. The vibrating tube is made of stainless steel and can work at pressures up to 40 MPa. The period of the vibration, τ , is recorded with a HP53131A data acquisition unit. The uncertainty of the vibrating period values is $\pm 10^{-8}$ s. The temperature of the vibrating tube is controlled by a regulated liquid bath (model: Lauda RE206) with a stability within ± 0.01 K. The temperature of the remaining parts of the circuit is regulated by a liquid bath (model: West P6100). Temperatures are measured by two Pt100 probes connected to the HP34970A data acquisition unit. These Pt100 probes are also periodically calibrated against a $25\ \Omega$ reference thermometer (model: Tinsley Precision Instrument) certified by the Laboratoire National d'Essais (Paris, France). Vacuum was achieved by means of a vacuum pump (model: AEG type LN38066008). Pressures are measured using two pressure transducers (model: Druck PTX611) with two complementary ranges: (0 to 3) MPa and (0 to 20) MPa. These sensors were calibrated against a dead weight pressure balance (model: Desgranges & Huot model 5202S) which has a (0.3 to 40) MPa pressure range and against an electronic balance (fundamental digital pressure standard, model: Desgranges & Huot 24610, France) for pressures below 0.3 MPa. The pressure transducers are connected to the HP34970A data acquisition unit.

Table 1. Pure Component Vapor Pressure for HFP

T/K	P/MPa	T/K	P/MPa
253.26	0.1497	328.21	1.5951
258.26	0.1841	333.21	1.7914
263.16	0.2245	338.18	2.0079
268.24	0.2720	343.21	2.2438
273.24	0.3268	348.22	2.5005
278.21	0.3890	353.23	2.7823
278.22	0.3886	355.24	2.9030
283.23	0.4590	356.24	2.9653
288.21	0.5371	356.76	2.9985
293.19	0.6259	357.06	3.0175
298.22	0.7283	357.27	3.0310
303.22	0.8397	357.47	3.0442
308.21	0.9634	357.56	3.0504
313.21	1.0999	358.26	3.0951
318.22	1.2506	358.76	3.1281
323.20	1.4135		

Materials. HFP was supplied by NECSA (South African Nuclear Energy Corporation) with a certified purity higher than 0.9999 volume fraction. Gas chromatographic analysis of the sample indicated a single component peak and therefore qualitatively verified the purity.

Experimental Procedure. Details concerning the experimental procedure are fully described in previous papers.³ As it is a dynamic method, we take care by reducing the flow close to the critical point to cancel the effect of fluctuations of the state variable in this region. The forced path mechanical calibration model (FPMC method) proposed by Bouchot and Richon⁸ is used to convert periods into density values. FPMC parameters were calculated from data (PVT) of a reference fluid (R134a), whose thermodynamic properties are well-described by the equation of state of Tillner-Roth and Baehr.⁹

Estimation of Uncertainties. The total uncertainty on density data in the vapor and liquid phases is estimated to be $\pm 0.05\%$, because of the uncertainties of the mechanical parameters used in the FPMC model. Total temperature uncertainties are estimated to be $\pm 0.02\text{ K}$. Total uncertainties on pressure measurements after calibration are (± 0.0003 and ± 0.0006) MPa, respectively, for the sensor range (3 and 20) MPa.

Experimental Results

Vapor Pressure. Table 1 shows the results for pure-component vapor pressures. The temperature range for measurements was from (253.26 to 358.76) K. The values of critical temperature and pressure were determined by experimental means. The critical point was observed with the disappearance of the vapor–liquid interface and critical opalescence in the cell. From this observation, it was determined that $T_C = (358.8 \pm 0.1)\text{ K}$ and $P_C = (3.129 \pm 0.001)\text{ MPa}$. The measured vapor-

pressure data were used to fit the parameters of the Frost–Kalkwarf¹⁰ equation (see eq 1). The average absolute relative deviation is less than 0.2 %, and the bias is -0.07% (see Figure 1).

$$P/\text{Pa} = \exp\left(A + \frac{B}{(T/\text{K})} + C \ln(T/\text{K}) + D \cdot 10^{-17} \cdot (T/\text{K})^E\right) \quad (1)$$

where P is the pressure, T is the temperature, and A , B , C , D , and E are adjustable parameters with values of 51.9463, -3799.9997, -4.5245, 10.1553, and 6, respectively.

There exists some literature data for vapor pressure which has been previously measured by Li et al.,¹¹ but their vapor pressure values are inconsistent with our measurements. We have undertaken measurements of vapor pressure independently on three separate occasions in our laboratories in France and South Africa and obtained the same results, using two separate samples of HFP. It is therefore our opinion that the data in literature are probably unreliable.

Densities. Tables 2 and 3 present our experimental results for temperatures between (263 and 362) K. Please note that this is not the full set of data measured, but a selection of points. The full data set is available in the supplementary data file. Tables 4 shows the densities determined at saturation in the (0 to 10) MPa pressure range considering the vapor pressure and the previously measured densities. The densities at saturation were used to determine the critical properties of the pure component. Two laws can be used for the determination of critical temperature T_C and critical density ρ_C . The first is a scaling law directly related to the difference of densities between the vapor and the liquid phase (eq 2) and expressed as follows:

$$\rho^L - \rho^V = A(T - T_C)^\beta \quad (2)$$

where β is an universal exponent constant (0.325). It is also assumed that the densities of the coexisting liquid and vapor obey the law of rectilinear diameters (eq 3) given as:

$$\frac{\rho^L + \rho^V}{2} = B(T - T_C) + \rho_C \quad (3)$$

where ρ^L ($\text{kg}\cdot\text{m}^{-3}$) and ρ^V ($\text{kg}\cdot\text{m}^{-3}$) are liquid and vapor densities, respectively. A ($\text{kg}\cdot\text{m}^{-3}\cdot\text{K}^{-\beta}$) and B ($\text{kg}\cdot\text{m}^{-3}\cdot\text{K}$) are adjustable parameters. The corresponding values are presented in Table 5, along with the critical properties of HFP (including acentric factor). The uncertainties on temperature and pressure are $\pm 0.1\text{ K}$ and $\pm 0.001\text{ MPa}$, respectively. Figures 2 and 3 show the $P-\rho$ diagram, including the critical point. Using eqs 2 and 3, one can obtain eqs 4 and 5 for the determination of vapor and liquid densities at saturation as follows:

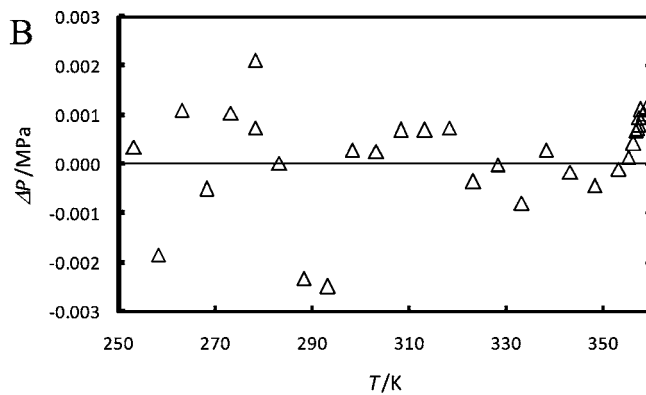
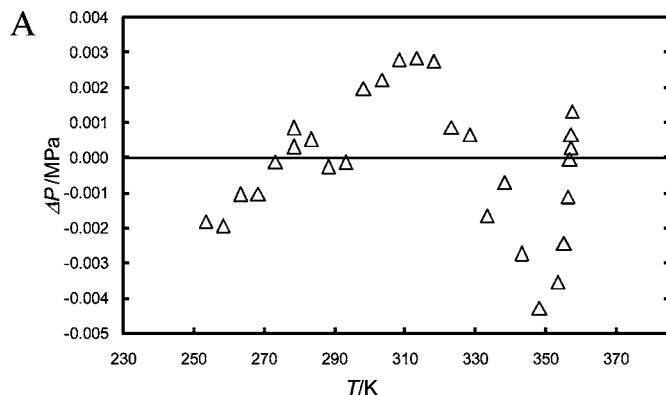


Figure 1. Deviation between the calculated vapor pressure and the experimental one; A, Frost–Kalkwarf equation; B, Wagner equation.

Table 2. Vapor Densities of HFP

<i>P</i>	<i>P</i>	<i>P</i>	<i>P</i>	<i>P</i>	<i>P</i>	<i>P</i>	<i>P</i>
MPa	kg·m ⁻³	MPa	kg·m ⁻³	MPa	kg·m ⁻³	MPa	kg·m ⁻³
<i>T/K = 263.41</i>							
0.0009	0.03	0.0507	3.48	0.1142	8.06	0.1899	13.87
0.0029	0.15	0.0561	3.85	0.1196	8.49	0.1957	14.37
0.0057	0.35	0.0614	4.28	0.1244	8.88	0.2013	14.81
0.0085	0.55	0.0667	4.62	0.1302	9.28	0.2069	15.26
0.0093	0.61	0.0680	4.73	0.1318	9.44	0.2083	15.38
0.0100	0.66	0.0693	4.82	0.1330	9.50	0.2096	15.49
0.0107	0.71	0.0705	4.89	0.1347	9.61	0.2110	15.60
0.0114	0.79	0.0713	4.97	0.1364	9.79	0.2123	15.71
0.0144	0.96	0.0764	5.28	0.1432	10.31	0.2176	16.16
0.0171	1.17	0.0816	5.72	0.1498	10.80	0.2211	16.43
0.0215	1.40	0.0860	6.00	0.1563	11.29	0.2232	16.59
0.0272	1.83	0.0910	6.41	0.1627	11.79		
0.0328	2.25	0.0960	6.75	0.1686	12.22		
0.0377	2.61	0.1004	7.07	0.1748	12.73		
0.0432	2.95	0.1058	7.51	0.1809	13.22		
0.0480	3.31	0.1107	7.85	0.1869	13.66		
0.0494	3.40	0.1124	7.99	0.1884	13.77		
<i>T/K = 263.41</i>							
0.0036	0.14	0.0693	4.38	0.2033	13.55	0.3409	23.85
0.0060	0.30	0.0812	5.20	0.2133	14.30	0.3539	24.84
0.0098	0.52	0.0934	6.00	0.2233	14.99	0.3667	25.93
0.0134	0.85	0.1044	6.69	0.2323	15.69	0.3795	26.94
0.0170	0.98	0.1140	7.35	0.2423	16.38	0.3923	27.96
0.0215	1.25	0.1236	8.03	0.2523	17.15	0.4050	28.98
0.0263	1.57	0.1334	8.66	0.2630	17.89	0.4177	30.05
0.0312	1.87	0.1457	9.54	0.2729	18.60	0.4303	31.07
0.0363	2.23	0.1556	10.24	0.2831	19.39	0.4429	32.26
0.0414	2.51	0.1651	10.87	0.2937	20.20	0.4544	33.16
<i>T/K = 263.41</i>							
0.0024	0.14	0.1242	7.43	0.3090	19.54	0.5977	41.02
0.0110	0.59	0.1373	8.36	0.3257	20.70	0.6256	43.25
0.0163	0.86	0.1478	9.01	0.3462	22.19	0.6507	45.35
0.0245	1.40	0.1637	9.96	0.3669	23.58	0.6705	47.07
0.0336	1.94	0.1740	10.66	0.3875	25.04	0.6900	48.67
0.0418	2.46	0.1844	11.32	0.4069	26.42	0.7189	51.33
0.0525	3.04	0.2028	12.46	0.4357	28.54	0.7461	53.68
0.0614	3.61	0.2164	13.34	0.4574	30.13	0.7741	56.30
0.0683	3.99	0.2303	14.30	0.4777	31.60	0.7969	58.41
0.0812	4.80	0.2512	15.74	0.5096	33.97	0.8236	61.02
<i>T/K = 303.28</i>							
0.0024	0.14	0.1242	7.43	0.3090	19.54	0.5977	41.02
0.0110	0.59	0.1373	8.36	0.3257	20.70	0.6256	43.25
0.0163	0.86	0.1478	9.01	0.3462	22.19	0.6507	45.35
0.0245	1.40	0.1637	9.96	0.3669	23.58	0.6705	47.07
0.0336	1.94	0.1740	10.66	0.3875	25.04	0.6900	48.67
0.0418	2.46	0.1844	11.32	0.4069	26.42	0.7189	51.33
0.0525	3.04	0.2028	12.46	0.4357	28.54	0.7461	53.68
0.0614	3.61	0.2164	13.34	0.4574	30.13	0.7741	56.30
0.0683	3.99	0.2303	14.30	0.4777	31.60	0.7969	58.41
0.0812	4.80	0.2512	15.74	0.5096	33.97	0.8236	61.02
<i>T/K = 303.28</i>							
0.0070	0.29	0.1958	11.28	0.4044	24.26	0.9791	66.90
0.0217	1.12	0.2111	12.24	0.4206	25.28	1.0261	71.06
0.0366	2.07	0.2264	13.16	0.4444	26.88	1.0718	75.20
0.0516	2.99	0.2414	14.08	0.5104	31.18	1.1207	80.05
0.0661	3.74	0.2603	15.25	0.5556	34.31	1.1657	84.23
0.0802	4.49	0.2806	16.35	0.5997	37.33	1.2116	88.92
0.0944	5.41	0.2971	17.47	0.6430	40.40	1.2549	93.54
0.1125	6.44	0.3139	18.45	0.6872	43.61	1.2987	98.44
0.1267	7.23	0.3303	19.52	0.7355	47.22	1.3475	104.06
0.1416	8.08	0.3470	20.58	0.7846	50.99	1.3925	109.80
<i>T/K = 323.21</i>							
0.0070	0.29	0.1958	11.28	0.4044	24.26	0.9791	66.90
0.0217	1.12	0.2111	12.24	0.4206	25.28	1.0261	71.06
0.0366	2.07	0.2264	13.16	0.4444	26.88	1.0718	75.20
0.0516	2.99	0.2414	14.08	0.5104	31.18	1.1207	80.05
0.0661	3.74	0.2603	15.25	0.5556	34.31	1.1657	84.23
0.0802	4.49	0.2806	16.35	0.5997	37.33	1.2116	88.92
0.0944	5.41	0.2971	17.47	0.6430	40.40	1.2549	93.54
0.1125	6.44	0.3139	18.45	0.6872	43.61	1.2987	98.44
0.1267	7.23	0.3303	19.52	0.7355	47.22	1.3475	104.06
0.1416	8.08	0.3470	20.58	0.7846	50.99	1.3925	109.80
<i>T/K = 343.26</i>							
0.0032	0.22	0.2005	11.16	0.8502	51.23	1.5621	109.24
0.0121	0.73	0.2505	14.05	0.9022	54.71	1.6692	120.33
0.0224	1.29	0.2983	16.80	0.9540	58.46	1.7733	132.05
0.0320	1.75	0.3477	19.66	1.0082	62.31	1.8809	145.46
0.0399	2.11	0.3965	22.56	1.0603	66.22	1.9861	160.18
0.0554	3.00	0.4433	25.35	1.1156	70.43	2.0963	177.82
0.0708	3.87	0.4909	28.19	1.1703	74.72	2.1724	192.40
0.0801	4.42	0.5486	31.65	1.2311	79.48	2.2377	208.04
0.0899	4.91	0.6044	35.15	1.2903	84.46	2.2417	211.34
0.1101	6.10	0.6603	38.68	1.3472	89.34		
0.1355	7.51	0.7156	42.26	1.4037	94.34		
0.1609	8.89	0.7705	45.84	1.4587	99.32		
0.1896	10.49	0.8239	49.41	1.5111	104.29		
<i>T/K = 348.12</i>							
0.0024	0.05	0.1869	9.89	0.7655	44.05	1.6838	116.62
0.0054	0.18	0.2089	10.99	0.8447	49.34	1.7806	126.81
0.0089	0.35	0.2452	13.05	0.9156	54.20	1.8729	137.09
0.0170	0.83	0.2810	15.00	0.9858	58.92	1.9679	148.35
0.0277	1.44	0.3175	17.06	1.0578	64.05	2.0685	161.51
0.0367	1.87	0.3522	19.05	1.1386	69.96	2.2121	183.28
0.0465	2.39	0.3865	20.98	1.2018	74.83	2.3102	201.01
0.0626	3.24	0.4201	22.92	1.2651	79.72	2.3973	219.85
0.0789	4.06	0.4709	25.92	1.3304	84.96	2.4728	240.22
0.0959	4.89	0.5280	29.29	1.3953	90.32	2.4815	242.88
0.1211	6.31	0.5912	33.18	1.4603	95.93	2.4901	245.80
0.1516	7.92	0.6721	38.15	1.5401	103.11	2.4988	250.42
0.1760	9.23	0.7358	42.16	1.6393	112.32		

Table 2. Continued

<i>P</i>	<i>P</i>	<i>P</i>	<i>P</i>	<i>P</i>	<i>P</i>	<i>P</i>	<i>P</i>
MPa	kg·m ⁻³	MPa	kg·m ⁻³	MPa	kg·m ⁻³	MPa	kg·m ⁻³
<i>T/K = 353.12</i>							
0.0008	0.029	0.4759	25.82	1.0237	60.42	2.0275	148.08
0.0143	0.737	0.4997	27.22	1.0858	64.72	2.1025	157.14
0.0288	1.442	0.5241	28.50	1.1468	69.00	2.1752	166.51
0.1019	5.291	0.5451	30.00	1.2476	76.44	2.2584	178.08
0.1407	7.318	0.6136	34.14	1.3303	82.80	2.3293	188.76
0.1803	9.389	0.6601	36.92	1.4342	91.01	2.3935	199.32
0.2204	11.538	0.7066	39.74	1.5313	99.10	2.4630	211.98
0.2628	13.844	0.7525	42.62	1.6215	106.97	2.5404	228.04
0.3221	17.107	0.8167	46.73	1.7051	114.65	2.6051	243.48
0.3587	19.177	0.8546	49.09	1.7830	122.06	2.6704	261.98
0.3988	21.420	0.8901	51.44	1.8719	130.23	2.7383	278.85
0.4182	22.524	0.9248	53.65	1.9218	136.34	2.7448	290.14
0.4658	25.243	0.9922	58.29	1.9901	143.83	2.7717	303.81
<i>T/K = 355.27</i>							
0.0017	0.10	0.1759	9.29	0.1054	61.79	2.1353	157.72
0.0048	0.28	0.2296	12.15	0.1409	67.89	2.2240	168.96
0.0088	0.47	0.2828	15.02	0.1226	74.03	2.3125	181.0

Table 3. Liquid Densities of HFP

<i>P</i>	<i>p</i>	<i>P</i>	<i>p</i>	<i>P</i>	<i>p</i>	<i>P</i>	<i>p</i>
MPa	kg·m ⁻³	MPa	kg·m ⁻³	MPa	kg·m ⁻³	MPa	kg·m ⁻³
<i>T/K = 263.49</i>							
0.2302	1462.58	0.7721	1465.47	2.8485	1475.67	6.2924	1491.15
0.2321	1462.66	0.8883	1465.94	3.0933	1476.76	6.6284	1492.50
0.2506	1462.76	0.9829	1466.54	3.3273	1477.91	6.9654	1493.98
0.2739	1462.91	1.1328	1467.28	3.5582	1479.03	7.3151	1495.44
0.3272	1463.13	1.2832	1467.96	3.7965	1480.12	7.6630	1496.86
0.3459	1463.25	1.4253	1468.74	4.0109	1481.02	8.0082	1498.24
0.3880	1463.45	1.5764	1469.48	4.2612	1482.25	8.3430	1499.65
0.4311	1463.65	1.7182	1470.09	4.5075	1483.36	8.6870	1500.96
0.4841	1463.94	1.8735	1471.02	4.7570	1484.43	9.0334	1502.38
0.5182	1464.18	2.0176	1471.69	5.1048	1485.97	9.3717	1503.79
0.5541	1464.39	2.2520	1472.79	5.4563	1487.53	9.5889	1504.56
0.6252	1464.59	2.4891	1474.06	5.7933	1489.06	9.7603	1505.19
0.7283	1465.20	2.7334	1475.13	6.1299	1490.42	9.9337	1505.89
0.7512	1465.25	2.7905	1475.34	6.2108	1490.70	9.9766	1506.02
<i>T/K = 283.17</i>							
0.4677	1382.09	1.7209	1391.22	4.4099	1408.82	7.7803	1428.05
0.4830	1382.29	1.8950	1392.44	4.6761	1410.42	8.0530	1429.55
0.5268	1382.57	2.0763	1393.62	4.8895	1411.65	8.2222	1430.51
0.5740	1382.98	2.3062	1395.23	5.1263	1413.10	8.3934	1431.32
0.6629	1383.60	2.5066	1396.64	5.3727	1414.61	8.5634	1432.23
0.7519	1384.27	2.6840	1397.73	5.7202	1416.66	8.7357	1433.12
0.8563	1384.98	2.9004	1399.13	5.9972	1418.20	8.9123	1434.00
0.9456	1385.66	3.1802	1400.96	6.2609	1419.73	9.0904	1435.02
1.0474	1386.36	3.3942	1402.39	6.5315	1421.22	9.2610	1435.85
1.1651	1387.20	3.5914	1403.66	6.8020	1422.82	9.4390	1436.78
1.3208	1388.36	3.8643	1405.48	7.0853	1424.29	9.6122	1437.57
1.4635	1389.43	4.0785	1406.71	7.3596	1425.90	9.7780	1438.42
1.6346	1390.61	4.2934	1408.17	7.6347	1427.34	9.9911	1439.48
<i>T/K = 303.36</i>							
0.8517	1288.08	1.3402	1293.72	3.0229	1311.53	5.9216	1337.37
0.8700	1288.22	1.4489	1294.92	3.1503	1312.98	6.1699	1339.47
0.8877	1288.47	1.5403	1296.17	3.2767	1313.98	6.4870	1341.93
0.9183	1288.76	1.6372	1297.09	3.4014	1315.17	6.7420	1343.99
0.9434	1289.10	1.7710	1298.55	3.5329	1316.48	7.0538	1346.25
0.9655	1289.39	1.8617	1299.58	3.7996	1319.05	7.3085	1348.26
0.9956	1289.74	1.9856	1301.03	4.0681	1321.53	7.5636	1350.15
1.0213	1290.00	2.1191	1302.35	4.3849	1324.43	7.8797	1352.39
1.0634	1290.50	2.3260	1304.46	4.6529	1326.85	8.2906	1355.42
1.1063	1291.06	2.4451	1305.96	4.8618	1328.62	8.7685	1358.79
1.1747	1291.89	2.5852	1307.14	5.0881	1330.55	9.1681	1361.57
1.2350	1292.43	2.8080	1309.41	5.4787	1333.80	9.6673	1364.90
1.3056	1293.27	2.9403	1310.77	5.7313	1335.77	9.9926	1366.98
<i>T/K = 323.37</i>							
1.4194	1174.23	2.2771	1192.28	4.2039	1224.27	6.8379	1257.77
1.4271	1174.45	2.3967	1194.59	4.3650	1226.67	7.0672	1260.31
1.4457	1175.00	2.5112	1196.77	4.5108	1228.65	7.2995	1262.75
1.4972	1176.12	2.6713	1199.65	4.7275	1231.69	7.5314	1265.19
1.5497	1177.31	2.8332	1202.46	4.9384	1234.66	7.7647	1267.63
1.6060	1178.65	2.9892	1205.13	5.1557	1237.37	7.9955	1270.08
1.6653	1179.86	3.1485	1207.95	5.3860	1240.28	8.2779	1272.98
1.7186	1180.95	3.3193	1210.67	5.5755	1242.70	8.5653	1275.71
1.7973	1182.59	3.4943	1213.56	5.8081	1245.67	8.8715	1278.77
1.8974	1184.74	3.6555	1215.99	6.0350	1248.49	9.1280	1281.22
1.9888	1186.54	3.8142	1218.51	6.2654	1251.23	9.4048	1283.76
2.1026	1188.84	3.9683	1220.84	6.4946	1253.91	9.6829	1286.27
2.2133	1191.16	4.1259	1223.19	6.7214	1256.27	9.9863	1289.02
<i>T/K = 343.18</i>							
2.2571	1022.11	2.8871	1056.99	4.6976	1116.51	7.4775	1171.63
2.2792	1024.07	2.9674	1060.20	4.8874	1121.18	7.6634	1174.54
2.3140	1026.50	3.0782	1064.77	5.0739	1125.85	7.8376	1177.31
2.3486	1028.71	3.2019	1069.74	5.3019	1130.82	8.0431	1180.22
2.3867	1030.85	3.3320	1075.03	5.4740	1134.83	8.2915	1184.04
2.4264	1032.67	3.4633	1079.82	5.7021	1139.38	8.4648	1186.51
2.4640	1034.92	3.5866	1084.11	5.8913	1143.58	8.6707	1189.47
2.4971	1037.07	3.7282	1089.03	6.1600	1148.79	8.8812	1192.40
2.5568	1040.31	3.8825	1093.89	6.4073	1153.32	9.1234	1195.43
2.6329	1044.34	4.0492	1099.28	6.7259	1159.01	9.3501	1198.56
2.7106	1048.77	4.2269	1104.11	6.9766	1163.25	9.5675	1201.28
2.7821	1051.54	4.4108	1109.10	7.1637	1166.50	9.7499	1203.76
2.8522	1055.00	4.5991	1114.05	7.3547	1169.81	9.9626	1206.45
<i>T/K = 348.16</i>							
2.5064	959.60	2.8351	989.69	4.0308	1052.17	7.1428	1134.61
2.5107	960.12	2.8885	993.69	4.2787	1061.59	7.3962	1139.31
2.5170	960.83	2.9691	999.28	4.5260	1070.05	7.6468	1143.93
2.5226	961.35	3.0615	1005.54	4.7760	1077.88	7.8977	1148.36
2.5322	962.81	3.1352	1009.88	5.0226	1085.31	8.1497	1152.67
2.5423	963.60	3.2025	1013.88	5.2672	1091.82	8.4063	1157.00
2.5545	964.95	3.2870	1018.73	5.5133	1098.50	8.6597	1160.84
2.5817	967.68	3.3306	1020.95	5.7622	1104.69	8.9117	1164.85
2.6147	970.90	3.3593	1022.61	6.0125	1110.68	9.1703	1168.80
2.6547	974.76	3.3862	1023.86	6.2622	1116.40	9.3994	1172.31
2.7061	979.32	3.4508	1027.09	6.5177	1121.84	9.6096	1175.39
2.7569	983.71	3.6201	1035.16	6.7677	1127.07	9.7889	1175.42
2.8094	987.97	3.8755	1046.10	7.0175	1132.05	10.0158	1180.60

Table 3. Continued

<i>P</i>	<i>p</i>	<i>P</i>	<i>p</i>	<i>P</i>	<i>p</i>	<i>P</i>	<i>p</i>
MPa	kg·m ⁻³	MPa	kg·m ⁻³	MPa	kg·m ⁻³	MPa	kg·m ⁻³
<i>T/K = 353.13</i>							
2.7984	887.06	3.7360	988.50	5.5598	1065.32	7.5217	1113.95
2.8257	893.67	3.8407	994.81	5.7117	1069.91	7.7198	1117.99
2.8526	899.46	3.9437	1000.71	5.8654	1074.15	7.9258	1122.03
2.8810	904.67	4.0667	1007.14	6.0196	1078.56	8.1280	1125.99
2.9482	915.77	4.2160	1014.76	6.1779	1082.78	8.3333	1129.80
3.0305	926.96	4.3743	1022.01	6.3335	1086.90	8.5330	1133.60
3.1161	937.73	4.5340	1028.89	6.4846	1090.62	8.7394	1137.27
3.2055	946.93	4.6920	1035.33	6.6427	1094.43	8.9409	1140.78
3.2863	954.54	4.8549	1041.63	6.8028	1098.22	9.1445	1144.29
3.3692	961.77	5.0121	1047.29	6.9608	1101.88	9.3534	1147.68
<i>T/K = 355.18</i>							
2.9179	845.60	3.4534	937.53	4.8739	1023.70	7.3662	1097.33
2.9277	849.49	3.5605	947.64	5.0298	1029.94	7.5663	1101.91
2.9369	852.80	3.6672	956.48	5.2368	1037.65	7.8173	1107.12
2.9466	855.85	3.7516	963.12	5.3987	1043.42	8.0691	1112.30
2.9677	861.92	3.8289	968.54	5.6014	1050.18	8.2739	1116.30
3.0045	872.46	3.9389	976.09	5.7682	1055.50	8.4785	1120.28
3.0399	880.60	4.0336	981.94	5.9355	1060.51	8.6815	1124.00
3.1369	887.86	4.1298	987.54	6.1732	1067.09	8.8868	1127.78
3.1787	904.31	4.2068	992.10	6.3624	1072.65	9.1381	1132.17
3.2122	910.46	4.2818	995.99	6.6115	1079.21	9.3393	1135.60
3.2731	917.41	4.4498	1004.57	6.8128	1084.30	9.5929	1139.78

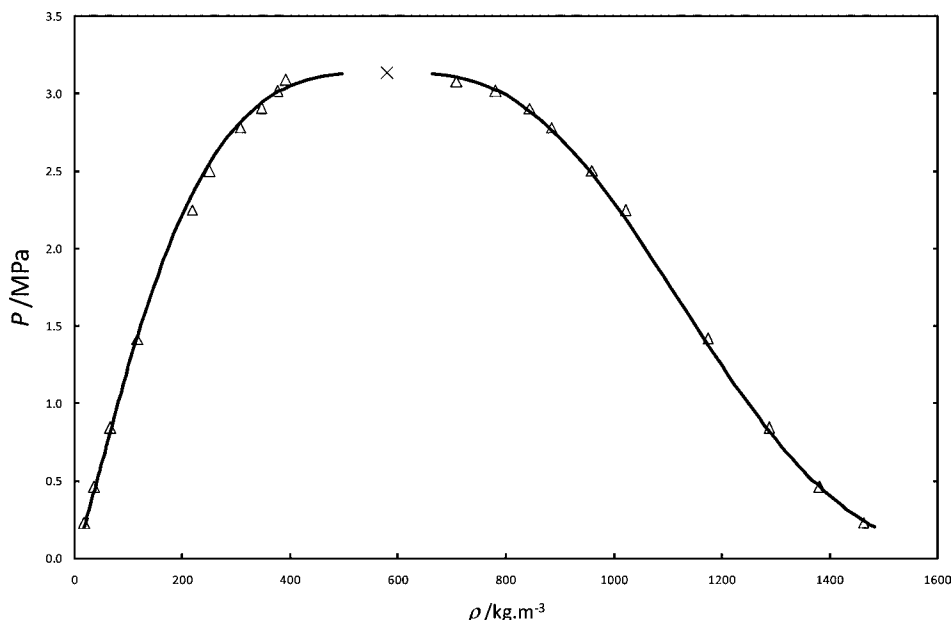


Figure 2. HFP $P-\rho$ diagram. Δ , experimental densities; \times , critical point; black line, calculated densities using eqs 4 and 5.

Table 4. Vapor and Liquid Densities at Saturation

vapor phase			liquid phase			
T	P	ρ^V	T	P	ρ^L	$\Delta\rho^{La}$
K	MPa	$\text{kg} \cdot \text{m}^{-3}$	K	MPa	$\text{kg} \cdot \text{m}^{-3}$	
263.41	0.2277	17.0	± 0.2	263.49	0.2284	1462.6 ± 0.2
283.24	0.4586	35.7	± 0.1	283.17	0.4576	1382.1 ± 0.2
303.28	0.8389	65.2	± 0.1	303.36	0.8408	1288.0 ± 0.2
323.21	1.4130	116.3	± 0.2	323.37	1.4186	1174.2 ± 0.3
343.26	2.2490	217.2	± 0.4	343.18	2.2451	1021.6 ± 0.6
348.12	2.4994	250.2	± 0.3	348.16	2.5016	959.3 ± 0.3
353.12	2.7794	306.7	± 1.0	353.13	2.7800	883.5 ± 1.0
355.27	2.9072	345.6	± 0.2	355.18	2.9018	844.0 ± 0.5
357.06	3.0172	375.6	± 0.2	357.01	3.0141	780.0 ± 0.2
358.16	3.0865	391.3	± 0.4	358.00	3.0763	708.0 ± 0.4

^a Estimated uncertainty due to density determination.

$$\ln\left(\frac{P}{P_C}\right) = \frac{T_C}{T}(A_1\tau + A_2\tau^{1.5} + A_3\tau^3 + A_4\tau^6) \quad (6)$$

$$\text{with } \tau = 1 - \frac{T}{T_C}$$

Critical properties used are those obtained using our correlations (eqs 1 to 3). The data are well-correlated, and the parameters are presented in Table 6. The bias and average absolute deviation are 0.02 % and 0.08 %, respectively.

The PR EoS, which is the most-used equation of state in industry, with the Mathias–Copeman (MC)¹⁵ α function was also used to correlate the vapor-pressure data. The MC parameters (c_1 , c_2 , and c_3) are indicated in Table 6. The average

absolute relative deviation is less than 0.1 %, and bias is –0.01 % (see Figure 1).

Densities. The Span–Wagner EoS adapted to polar fluids was used to correlate the data. We have used the densities at saturation and the corresponding vapor pressure to determine the parameters.

$$\frac{A^\gamma}{RT} = \sum_1^{12} n_i \delta^{d_i} \tau^{t_i} \exp(e_i \delta^{p_i}) \quad (7)$$

$$\text{with } \tau = \frac{T_C}{T} \quad \text{and} \quad \delta = \frac{\rho}{\rho_C}$$

The parameters are presented in Table 6. The PR EoS is also used to compare the densities at saturation with the densities calculated with the Span–Wagner EoS and the experimental one (see Figure 4). The Span–Wagner EoS represents with some difficulties with our experimental data (there are 12 adjustable parameters), particularly close to the critical point. Figure 5 presents the pure-component vapor pressures. It seems that more data are required to generate a good equation of state. The Span–Wagner EoS determined different property values for the critical point ($T_C = 358.9$ K, $\rho_C = 589.5$ $\text{kg} \cdot \text{m}^{-3}$, and $P_C = 3.189$ MPa). We have tested also the PR EoS on the calculation of densities (Figure 4). As expected, the PR EoS is not accurate enough to represent the densities of the liquid phase at saturation. For this reason, the PR volume-translated EoS was also used to improve the representation of the densities, and it gave reasonable representation of both the liquid and the vapor densities at

Table 5. Pure-Component Critical Properties and Mathias–Copeman α Function Parameters

critical properties				Mathias–Copeman parameters			
T_C/K	P_C/MPa	$\rho_C/(\text{kg} \cdot \text{m}^{-3})$	Pitzer's acentric factor ω	Z_C	c_1	c_2	c_3
358.9	3.136	579.03	0.3529	0.27226	0.8926	-0.5100	3.1585
Eqs 4 and 5 Parameters							
A				B			
329.47				1.73			

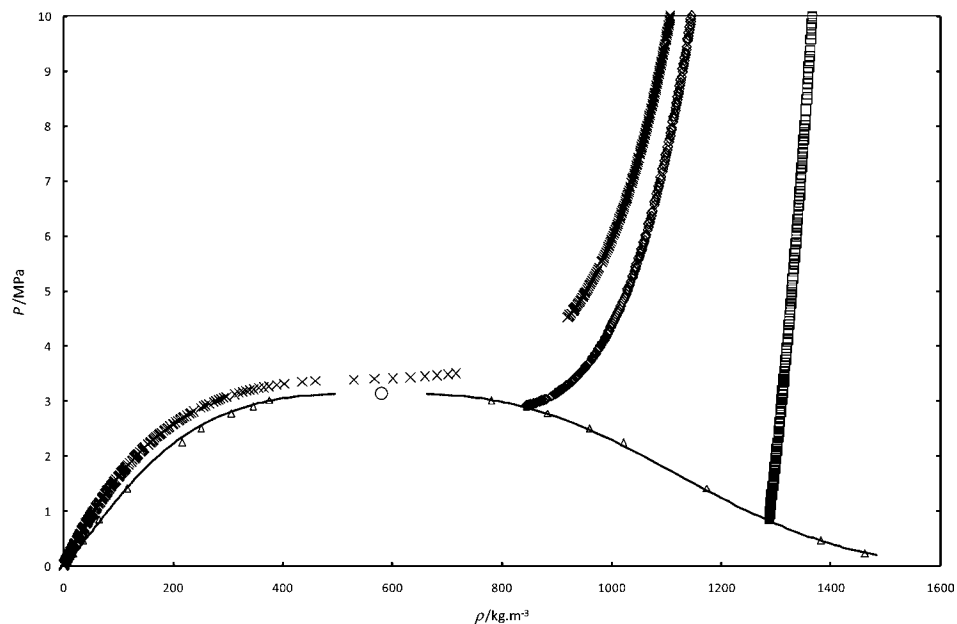


Figure 3. HFP $P-\rho$ diagram. Δ , experimental densities at saturation; \times , out of saturation; 362.90 K; \diamond , 355.18 K, and \square , 303.28 K; \circ , critical point; black line, eqs 4 and 5.

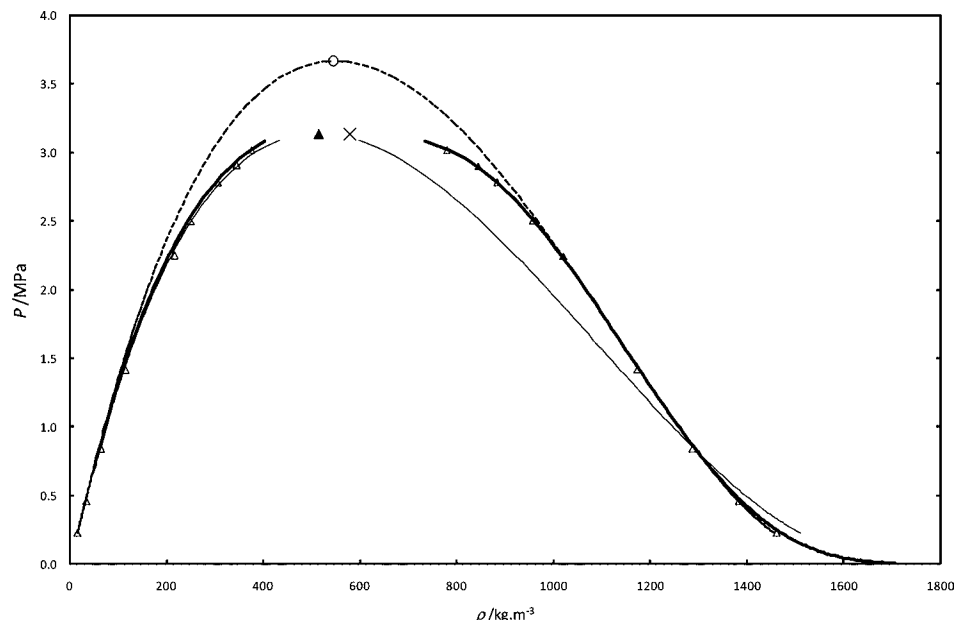


Figure 4. HFP $P-\rho$ diagram. Δ , experimental densities; \times , critical point from eqs 1 to 3; \circ , critical point obtained with the translated PR EoS; \blacktriangle , critical density obtained with the PR EoS; bold line, calculated densities with the Span-Wagner equation; black line, calculated densities using the PR EoS; dashed line, calculated using the translated PR EoS.

Table 6. Wagner and Span-Wagner Equation Parameters

i	Wagner equation		Span-Wagner equation				
	A_i	d_i	t_i	e_i	p_i	n_i	
1	-7.56784	1	0.25	0	0	1.06801	
2	1.31089	1	1.25	0	0	-2.69766	
3	-5.03405	1	1.5	0	0	0.431879	
4	0.60477	3	0.25	0	0	0.0846552	
5		7	0.875	0	0	0.00029316	
6		1	2.375	-1	1	0.566737	
7		2	2	-1	1	0.475546	
8		5	2.125	-1	1	-0.0390086	
9		1	3.5	-1	2	-0.447262	
10		1	6.5	-1	2	-0.0784903	
11		4	4.75	-1	2	-0.126779	
12		2	12.5	-1	3	0.00327112	

low pressures. Concerning the calculation at high pressure, it calculated values significantly higher than the “good” expected values for both phase densities particularly at pressures in the critical region. In fact, density data and pure-component vapor pressures were used to fit the equation of state parameters and critical properties. The estimated critical temperature and pressure are 367.20 K and 3.665 MPa, respectively. This calculation reveals that it is difficult to represent very accurately the thermodynamic properties in the vicinity of the critical point, and a specific model must be developed like those used by Anisimov and Sengers¹⁶ considering the asymptotic-scaled equation of state and renormalization theory.

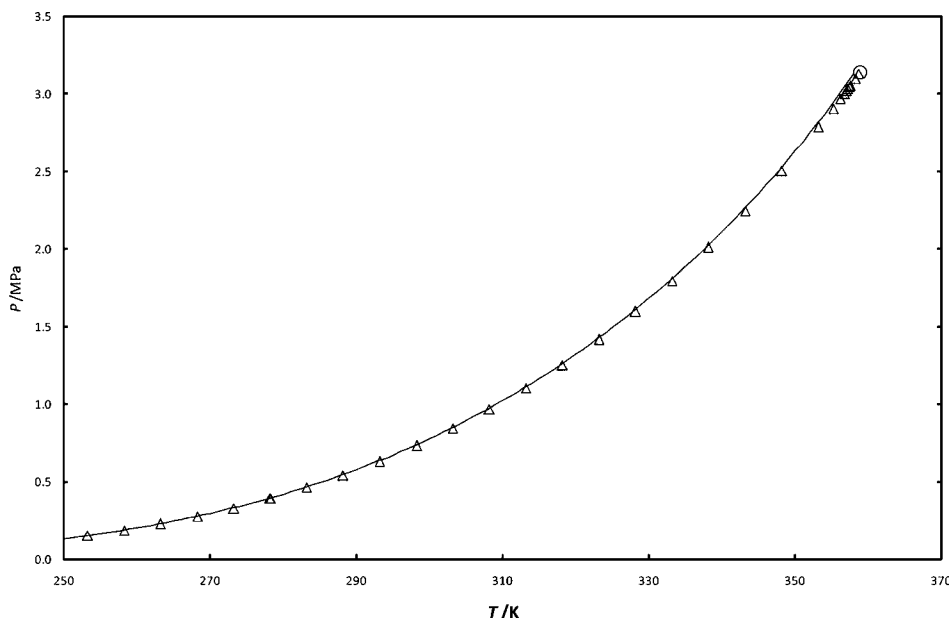


Figure 5. Pure HFP vapor pressure. Δ , experimental data; solid line, the Span–Wagner equation of state.

Conclusion

A vibrating-tube densitometer was used to determine the density of pure hexafluoropropylene. The uncertainties of the vapor and liquid densities were $\pm 0.05\%$ using the FPMC approach. Using these data, new values of critical properties were determined and validated through visual measurement on a static cell.

Supporting Information Available:

Vapor and liquid densities of HFP at various temperatures. This material is available free of charge via the Internet at <http://pubs.acs.org>.

Literature Cited

- (1) McMullan, J. T. Refrigeration and the environment issues and strategies for the future. *Int. J. Refrig.* **2002**, *25*, 89–99.
- (2) Acerboni, G.; Buekes, J. A.; Jensen, N. R.; Hjorth, J.; Myhre, G.; Nielsen, C. J.; Sundet, J. K. Atmospheric degradation and global warming potentials of three perfluoroalkenes. *Atmos. Environ.* **2001**, *35*, 4113–4123.
- (3) Bouchot, C.; Richon, D. Direct pressure-volume-temperature and vapor-liquid equilibrium measurements with a single equipment using a vibrating tube densimeter up to 393 K and 40 MPa: description of the original apparatus and new data. *Ind. Eng. Chem. Res.* **1998**, *37*, 3295–3304.
- (4) Peng, D. Y.; Robinson, D. B. A new two parameters Equation of State. *Ind. Eng. Chem. Fundam.* **1976**, *15*, 59–64.
- (5) Span, R.; Wagner, W. Equations of state for technical applications. III. Results for polar fluids. *Int. J. Thermophys.* **2003**, *24*, 111–161.
- (6) Peneloux, A.; Rauzy, E. A consistent correction for Redlich-Kwong-Soave volumes. *Fluid Phase Equilib.* **1982**, *8*, 7–23.
- (7) Coquelet, C.; Valtz, A.; Richon, D. Vapor - Liquid Equilibrium Data for the Difluoromethane (R32) + Dimethyl Ether (DME) System at Temperatures from 283.03 to 363.21 K and Pressures up to about 5.5 MPa. *Fluid Phase Equilib.* **2005**, *232*, 44–49.
- (8) Bouchot, C.; Richon, D. An enhanced method to calibrate vibrating tube densimeters. *Fluid Phase Equilib.* **2001**, *191*, 189–208.
- (9) Tillner-Roth, R.; Baehr, H. D. An international standard formulation for the properties of 1,1,1,2-tetrafluoroethane (HFC-R134a) for temperatures from 170 to 455 K and pressures up to 70 MPa. *J. Phys. Chem. Ref. Data* **1994**, *23*, 657–729.
- (10) Frost, A. A.; Kalkwarf, D. R. A semi-empirical equation for the vapor pressure of liquids as a function of temperature. *J. Chem. Phys.* **1953**, *21*, 264–267.
- (11) Li, C.; Feng, Y.; Wu, Z. Vapor pressure of hexafluoropropylene. *J. Chem. Eng. Chin. Univ.* **1996**, *10*, 64–66.
- (12) Dupont de Nemours, 2008. www.dupont.com/FluoroIntermediates/en_US/assets/downloads/h96536.pdf.
- (13) Daubert, T. E.; Danner, R. P.; Sibel, H. M.; Stebbins, C. C. *Physical and thermodynamic properties of pure chemicals*: Taylor & Francis: Washington, DC, 1997.
- (14) Wagner, W. New vapour pressure measurements for argon and nitrogen and a new method for establishing rational vapour pressure. *Cryogenics* **1973**, *13*, 470–482.
- (15) Mathias, P. M.; Copeman, T. W. Extension of The Peng Robinson Equation of State to Complex Mixtures: Evaluation of the Various Forms of the local Composition Concept. *Fluid Phase Equilib.* **1983**, *13*, 91–108.
- (16) Anisimov, M. A.; Sengers, J. V. *Equations of state for fluids and fluid mixtures*; Elsevier: Amsterdam, The Netherlands, 2000.

Received for review July 15, 2009. Accepted April 20, 2010.

JE900596D